JOURNAL OF PROPULSION AND POWER
Vol. 10, No. 6, Nov.–Dec. 1994

Coupling Between Vorticity and Pressure Oscillations in Combustion Instability

Habib N. Najm* and Ahmed F. Ghoniem†
Massachusetts Institute of Technology, Cambridge, Massachusetts 02139

The operation of premixed dump combustors is hindered by large-amplitude, low-frequency oscillations leading to flame flashback. The genesis of this instability is the subject of this article. A physical model that accounts for the relevant components of flow-combustion interactions in this system is formulated assuming that the combustor is an acoustically compact trough, the flow is two dimensional, the flame is a thin front, the inlet section is charged by a constant-pressure reservoir, and the exit pressure is forced. Numerical solutions at high Reynolds number are obtained using the vortex method. The nonreacting flow exhibits coherent oscillations that scale with the trough depth and inlet velocity to a Strouhal number of $\mathcal{O}(0.1)$. Simulations of the reacting flow show that vorticity-flame-acoustic coupling is the driving mechanism for the observed instability. In this work, the exit pressure is modulated near the frequency of the natural mode, and the amplitude of oscillation is observed to grow with increasing heat release due to phase-matched coupling between flow and heat release oscillations, in accordance with the Rayleigh criterion. This amplification ultimately leads to flow reversal and the propagation of the flame into the inlet channel.

Introduction

PREMIXED dump combustors exhibit an instability that manifests itself in low-frequency, large-amplitude flow, and pressure oscillations and the propagation of the flame upstream into the inlet duct. In this work, we investigate the dynamics of reacting flow in a cavity-type dump combustor to elucidate the mechanism of this "flashback" instability. Our objective is to understand the coupling between the dynamics of the recirculating flow in the dump and pressure oscillations in the combustor in the presence of heat release. The flashback we refer to here is not the conventional flashback[1] that involves upstream propagation of the flame in the boundary layer along solid walls due to small local convective velocities. Rather, as reported in the review of Plee and Mellor,[2] and observed in various controlled laboratory experiments,[3–5] this flashback is associated with convective flow reversal.

The detailed flow dynamics of nonreacting separating flow over a shallow cavity (or a backward-facing step) have been shown to exhibit large-scale vortex shedding at frequencies comparable to those in the wake behind bluff bodies, namely at $St = fD/U = \mathcal{O}(0.1)$, where D is the cavity/step depth, and U is the upstream channel flow velocity.[6–9] This wake-mode recirculation zone instability has been observed experimentally and in numerical modeling of the flowfield, and was shown to dominate the shear layer Kelvin-Helmholz instability for shallow cavities,[6] for which $L/D > 1$–2, where L is the cavity length.

Experimental results on premixed dump combustors have demonstrated that the large-scale organized recirculation zone eddy shedding observed in the nonreacting flow is also evident in the reacting case.[5] Schlieren photographs suggest that the flame is modulated by the large-scale vortex structures. The frequency spectra of the flow and pressure oscillations measured on these systems involve typically two or more frequency peaks, with the lower frequencies gaining dominance as the equivalence ratio, and therefore the rate of heat release is increased, and flashback is approached.[4,5]

The task of understanding the modes of oscillation corresponding to the above spectra has been tackled by many investigators. The complexity of the flow in these systems derives from the coupling between acoustics of the overall system and the convective dynamics and heat release in the combustor. Based on the Rayleigh criterion,[10] it is evident that significant amplification of the combustion system dynamics can occur when pressure and heat release oscillations are in-phase. However, the overall stability characteristics of a premixed dump combustion system are still the subject of investigation. Two outstanding issues are 1) what determines the oscillation modes of a given system, and 2) how does the system migrate between these modes when heat release is increased. The first item is the primary focus of this work. It has been suggested by some studies that this mode selection is determined by the acoustic characteristics of the combustor and the piping system.[7,11–13] This is based on the assertion that the acoustic power radiated from the unsteady flame feeds energy into the resonant acoustic modes of the system. The resonant pressure oscillations, which are fed back into the combustor, are believed to determine the frequency of the organized eddies shed from the shear layer and recirculation zone. While we agree in part with this scenario, we maintain that a significant body of experimental evidence[3,5,14–17] suggests that even if the higher modes of oscillation of the combustor correspond to specific acoustic modes of the system, the more dangerous low-frequency oscillation, which is the precursor to flashback, is generally observed to be in the St range (0.05–0.2), i.e., $St = \mathcal{O}(0.1)$. This suggests that this mode is determined by the dynamics of the recirculation zone. Thus, while the higher modes are "system" instabilities, the low-frequency mode that leads to flashback is a "combustor" instability in the sense that it is generally determined by the flow in the dump (the inlet flow speed and the depth of the dump) within a given Strouhal number range.

We therefore maintain that flashback occurs as a result of the amplification of the inherent recirculation zone instability, and that this amplification occurs as the pressure oscillation in the system approaches the natural frequency of the recirculation zone and as the rate of heat release at the flame is

Presented as Paper 89-2665 at the AIAA/ASME/SAE/ASEE 25th Joint Propulsion Conference, Monterey, CA, July 10–12, 1989; received Sept. 25, 1989; revision received March 14, 1994; accepted for publication April 7, 1994.

*Department of Mechanical Engineering; currently Senior Member of Technical Staff at Sandia National Labs, Livermore, CA 94551.

†Professor, Department of Mechanical Engineering. Associate Fellow AIAA.

increased. It has been demonstrated[18] under specific conditions of high-frequency forcing, where pressure oscillation at the natural low-frequency mode of the combustor is inhibited, that the dominant oscillation in the rate of heat release is decoupled from the prevalent high-frequency pressure oscillations; thus no Rayleigh-type amplification is observed upon increasing the heat release rate. In fact, the volume expansion due to heat release is seen to have a stabilizing influence similar to experimentally observed stabilization in external flows where pressure resonance is inhibited.[1] Furthermore, the experimental measurements of McManus et al.[16] demonstrate the stabilizing effect of high-frequency forcing. In the following we investigate the coupling between heat release and flow oscillation under low-frequency forcing, close to the natural wake mode of the recirculation zone. Significant amplification is observed, consistent with Rayleigh's criterion, leading to flame flashback into the upstream inlet.

Formulation and Numerical Scheme

A proper physical model of a premixed combustion system must include both local convective dynamics and extended acoustic dynamics. A typical experimental combustion system may be divided into three functionally distinct zones: 1) an upstream "reservoir," 2) a compact combustor, and 3) an exhaust system leading to the atmosphere.[18,19] In this work, only the upstream reservoir and the combustor are considered, as shown in Fig. 1. Neglecting the extended exhaust system removes a significant source of acoustic resonance in the overall combustion system. This source is substituted for in this work by externally imposed pressure forcing at the combustor exit. This allows the study of vorticity-flame-pressure coupling under controlled conditions.

Combustion is assumed to occur exclusively in the compact combustor zone, from $x_{\min}$ to $x_{\max}$ as shown in Fig. 1. Premixed reactants enter the combustor via the upstream channel at $x_{\min}$. They are expanded at the upstream step, where the flame is anchored and sustained by the recirculating hot products in the dump (cavity). Further downstream, the flow is constricted at the exit nozzle, at the downstream edge of the cavity, and the hot gases exit the combustor at $x_{\max}$.

The upstream flow is assumed to originate in an infinite reservoir at a stagnation pressure p_0. The model allows for both forward and reverse flow between the reservoir and the combustor, depending on the pressure at the combustor inlet.

The two zones are coupled at the inlet plane of the combustor, at $x_{\min}$. The instantaneous inlet flow rate for the combustor model is that calculated from the upstream reservoir model, while the pressure boundary condition for the reservoir model is provided by the upstream pressure in the combustor. The flow model and numerical solution for each zone are presented below.

Combustor

The dump combustor, or cavity, flow is modeled in two dimensions. The unsteady Navier-Stokes equations are solved with no turbulence modeling. As a consequence of the two-dimensional assumption, flow instabilities and vortex breakdown in the third dimension are not included in the model. While this does lead to more enhanced organization of the two-dimensional large-scale structures than is observed experimentally, previous results[6] have shown that the predicted flow oscillation frequencies and mean profiles fall well within the range of experimental observation. Furthermore, experimental evidence[3-5] demonstrates that the two-dimensional organization of large-scale structures is enhanced significantly in reacting flow, due to the system pressure resonances induced by the combustion process.

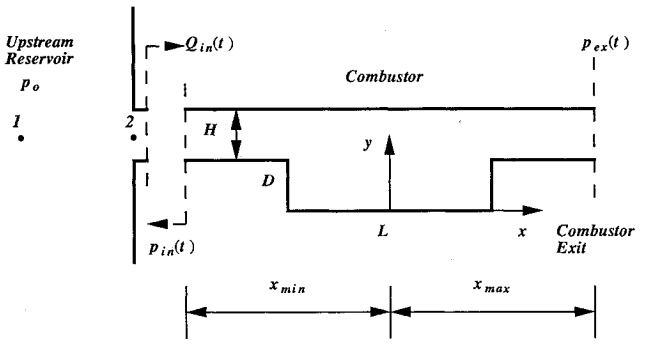

Fig. 1 Schematic diagram showing the combustor and upstream reservoir models.

The combustion model assumes a single-step, irreversible reaction[20] mechanism: $R \Rightarrow P$, where both reactants R and products P are considered to be perfect gases. Furthermore, a flamelet combustion regime is assumed,[21] with low flame stretch (turbulent Karlovitz number $K_a < 1$), and fast chemistry (turbulent Damkohler number $D_a > 1$). We also implement both the "low Mach number" and "thin flame" approximations.[22] The former is based on the assumption of an acoustically compact combustor, where the time scales associated with acoustic phenomena are negligible with respect to those relevant to convective flow dynamics. Whereas the latter, the thin flame approximation, takes the flamelet model to the limit by assuming a zero reaction zone thickness and a large activation energy.

The low Mach number assumption is justified for the subsonic experimental combustion systems of relevance here, where the combustion zone is a small component of a much larger inlet/exhaust piping system. The main result of this approximation is that the fluid is treated as an incompressible medium everywhere except at the flame. The justification of the flamelet and thin flame assumptions is also based on empirical evidence, where experimentally observed premixed combustor flow[3-5] suggests a distinct reaction zone/flame sheet that is relatively thin with respect to the large-scale flow structures.

Consequently, the flame is modeled as a surface of discontinuity between the reactants and the products, and combustion is allowed to occur only at the flame interface. The flame propagates by advection due to the local flow velocity, and by burning into the reactants normal to itself at a laminar burning velocity S_n, which depends on the local curvature of the flame surface.[23] Fluid density and temperature fields are uniform in the reactants and in the products with a discontinuity at the flame. Heat release at the flame front results in localized expansion of the fluid, which is modeled using discrete volume expansion sources along the flame interface.

Therefore, the low Mach number, thin flame, combustion model is a phenomenological scheme that involves no explicit chemical kinetics, but rather utilizes the end result of the chemical reaction in terms of the laminar flame speed and the density/temperature jump across the flame. Consequently, some characteristics of the combustion process, such as the transition between different reaction regimes or strain-induced flame extinction, are not included in the model. While these processes are of significant importance, they are not within the scope of this work.

Within the above framework, the fluid flow and combustion processes are coupled fundamentally by the expansion due to heat release at the flame, the advection of the flame by the flowfield, the change of fluid density and viscosity across the flame interface, and the baroclinic generation of vorticity at the flame.[24] Of these four mechanisms, the vorticity generation is deemed negligible in the present context, and is not included in the model. This is based on the expectation that this vorticity would only affect the local small-scale structure of the flame interface, and is therefore not of major interest to the present work.

Using the vorticity-stream function formulation, and the Helmholz decomposition[25] of the velocity field into a vortical

and an irrotational component, the governing equations based on the above model, written in dimensionless form, are[18]

$$\frac{D\omega}{Dt} = \frac{1}{Re}\nabla^2\omega \tag{1}$$

$$\boldsymbol{u} = \nabla\phi + \boldsymbol{u}_\omega \quad \text{and} \quad \boldsymbol{u}_\omega = \nabla \times \psi\boldsymbol{k} \tag{2}$$

$$\nabla^2\psi = -\omega \quad \text{and} \quad \nabla^2\phi = \frac{QS_u}{T_u}\delta(x - \chi_f) \tag{3}$$

$$\frac{d\chi_f}{dt} = \boldsymbol{u}_u(\chi_f) + S_u(\chi_f)\boldsymbol{n}_f \tag{4}$$

where $\omega\boldsymbol{k} = \nabla \times \boldsymbol{u}$ is the vorticity vector, Re is the Reynolds number, $\nabla\phi$ and $\boldsymbol{u}_\omega$ are the irrotational and vortical components of the velocity field, respectively, ψ and ϕ are the streamline and potential functions, respectively, Q is the enthalpy of reaction, S_u is the laminar burning speed with respect to the reactants, T_u is the temperature in the unburnt fluid (reactants), $[\chi_f(t)]$ is a set of points defining the flame interface at time t, $\boldsymbol{u}_u$ is the local fluid velocity in the vicinity of the flame interface—on the reactants side of the flame, and $\boldsymbol{n}_f$ is the local unit normal to the flame interface pointing towards the reactants. Furthermore, $(\rho, T, \mu) = (\rho_u, T_u, \mu_u)$ are the density, temperature, and viscosity in the reactants, and (ρ_b, T_b, μ_b) are defined similarly in the products, with $\rho_u T_u = \rho_b T_b$. The Reynolds number on either side of the flame is defined based on dimensional and reference quantities as follows: $Re = Re_u = \rho_u^* U_r^* D^*/\mu_u^*$ in the reactants, and $Re = Re_b = \rho_b^* U_r^* D^*/\mu_b^*$ in the products. The superscript * denotes a dimensional quantity, U_r^* is a nominal reference velocity, and D^* is the dimensional cavity depth and the reference length scale.

The dependence of the laminar burning speed S_u on the curvature of the flame interface is given by $S_u = S_n(1 - \Lambda/R_F)$, where S_n is the laminar burning speed of a planar flame, Λ is the Markstein length,[23] and R_F is the local radius of curvature of the flame interface.

The numerical solution of the above formulation is based on the random vortex method.[26,27] The vorticity field is discretized into a finite number of vortex elements that are generated at the walls to satisfy no-slip, and are advected and diffused in the flowfield according to the vorticity transport equation. A Lagrangian formulation is employed, whereby advection is expressed in terms of a set of coupled ordinary differential equations, whereas diffusion is simulated by an appropriate random walk algorithm.[26] Numerical diffusion is minimized by avoiding the discretization of velocity gradients on a grid. The scheme is grid-free and the computations are self-adaptive since vortex elements move to capture zones of large velocity gradients associated with concentrations of vorticity. The discretization of the continuous vorticity field into a finite number of vortex elements imposes a corresponding smallest resolvable length scale, whereas the time step used in updating the vorticity field imposes a minimum time scale. The accuracy of the method in two-dimensional high Reynolds number flow has been verified against experimental data.[6,28]

The flame interface is constructed and propagated on a uniform square grid using the simple line interface calculation (SLIC) algorithm,[29-31] coupled with the volume-of-fluid method (VOF).[32] The SLIC algorithm uses a set of horizontal and vertical straight line segments on a two-dimensional grid to construct the flame interface. The flame is propagated according to Eq. (4) using two fractional steps: 1) an advection step and 2) a burning step. Advection involves the motion of the flame interface as a passive material surface with the local flow velocity. Burning, on the other hand, involves the motion of the flame normal to itself into the reactants, at a laminar burning speed S_u, and is implemented using the classical Huyghens principle for wave front propagation.[18] The VOF method is used to generate a smoother flame interface from the SLIC data.

The combustor model requires a specification of the upstream inlet boundary condition, namely the volume flow rate $Q_{in}(t)$ into the inlet channel at each time step. This is computed from the upstream reservoir flow model discussed below. As will be demonstrated, this necessitates a specification of the pressure at the combustor exit $p_{ex}(t)$. Note, however, that the specification of $p_{ex}(t)$ is not directly imposed upon the combustor flow solution, rather it is used to solve the upstream reservoir one-dimensional Bernoulli equation to find $Q_{in}(t)$, which is then imposed at the combustor inlet x_{min}.

Upstream Reservoir

The model of the reservoir flow involves one of two incompressible flow problems, depending on the sign of the inlet flow rate. For $Q_{in}^{n-1} > 0$, i.e., for flow from the reservoir into the combustor, we solve the inviscid flow problem for the new flow rate Q_{in}^n, utilizing the unsteady Bernoulli integral written between points "1" and "2" shown in Fig. 1. The resulting equation, written in nondimensional form, is

$$\frac{p_1}{\rho_u} + \frac{\nu_1^2}{2} + \left(\frac{\partial\phi}{\partial t}\right)_1 = \frac{p_2}{\rho_u} + \frac{\nu_2^2}{2} + \left(\frac{\partial\phi}{\partial t}\right)_2 \tag{5}$$

The pressure at 1, which is at a large distance ($=50H$) from the channel entry, is assumed to be the fixed stagnation pressure $p_1 = p_0$, while the velocity $\boldsymbol{u}_1$ is assumed negligible, hence, $\nu_1 = |\boldsymbol{u}_1| = 0$. The pressure at 2, p_2, is that computed from the combustor flow field at x_{min} (Fig. 1). This is done by integrating the streamwise pressure gradient, $\partial p/\partial x$, along the channel centerline from x_{max} to x_{min}. The pressure at x_{max} is specified by the forcing function, while $\partial p/\partial x$ is computed at discrete points along the centerline, from the momentum equation, based on the prevailing flowfield. Hence, p_2 depends on the channel inlet flow rate Q_{in} through the combustor flow solution. Furthermore, $\boldsymbol{u}_2 = (\nu_2, 0)$, the velocity at point 2, is directly related to the inlet flow rate, and ϕ is the flow potential, such that $\boldsymbol{u}(x, t) = \nabla\phi(x, t)$. The determination of ϕ involves the solution of the Laplace equation, $\nabla^2\phi = 0$, for the flow geometry in the inlet section. This is easily done using Schwartz-Christoffel conformal mapping[33] to the upper half-plane, and the above equation can be simplified to the following ordinary differential equation[18]:

$$B\frac{dq}{dt} - \frac{A^2}{2}q^2 + \frac{p_0 - p_2}{\rho_u} = 0 \tag{6}$$

where A and B are constants related to the conformal mapping, q = channel inlet flow rate = Q_{in}, and $p_2 = p_2(q)$.

Equation (6) is solved for q^n using an implicit time discretization and Newton's iteration. Note that the only unknown is q^n, since $p_2^n = p_2(q^n)$. If q^n is found to have a negative value then the solution is repeated using the reverse flow formulation discussed below.

For the case of reverse flow, the upstream zone is modeled as a jet exiting into an infinite reservoir. The presence of the reservoir is enforced by setting the static pressure p_2 in the exiting jet to be equal to p_0. Hence, the reverse flow rate q^n is the solution of

$$p_2^n(q^n) = p_0 \tag{7}$$

Recall that p_2 is computed by integrating $\partial p/\partial x$ from x_{max} to x_{min}, and is a function of the vortical and expansion fields as well as the flow rate at the channel inlet q^n. Equation (7) is solved for q^n using Newton's iteration. Again, if q^n is found to be positive, then the flow has reversed to the downstream direction, and the solution is repeated using the forward flow formulation (6).

In each of these two cases, the value of p_2 is required from the flow inside the computational domain, between x_{min} and x_{max}, for a given inlet flow rate q. For each iteration, p_2 is found by integrating $\partial p/\partial x$ from the x-momentum equation from x_{max} to x_{min} along the channel centerline. Given that the velocity field is discontinuous at the flame interface, the discretization used for computing $\nabla \boldsymbol{u}$ and $\nabla^2 \boldsymbol{u}$ in the vicinity of the flame is one-sided, so as not to cross the discontinuity. The pressure jump across the flame discontinuity,[34] given by $\delta p_f = \rho_u S_u^2(\rho_u/\rho_b - 1)$, is taken into account in the computation of the pressure integral when the flame intersects the integration path.

Results and Discussion

The combustion tunnel is shown in Fig. 1. It consists of an infinite, constant-pressure reservoir, and a cavity-type dump combustor. The values of reference quantities are as follows. Reference density and viscosity are those of the reactants $\rho_r^* = 1.2$ kg/m^3, and $\mu_r^* = 2.0 \times 10^{-5}$ Ns/m^2, the reference length is the cavity depth $D^* = 2.5$ cm, the reference velocity is $U_r^* = 6.67$ m/s, and the reference gauge pressure is $p_r^* = \rho_r^*(U_r^*)^2 = 53.33$ Pa (gauge pressures are measured with respect to atmospheric pressure, $p_{atm}^* = 10^5$ Pa). Reference time is $t_r^* = D^*/U_r^*$. All quantities without the superscript * referred to below are normalized with the above reference quantities. Similarly, all quantities plotted in the figures are nondimensionalized accordingly.

The time-averaged mean inlet velocity in the upstream channel is $U = U^*/U_r^*$, where $U^* = (Q_{in}^*)_{av}/H^*$. This quantity U is found to lie in the range 0.44–0.84, in the results reported here. The Reynolds number introduced above in Eq. (1) is based on U_r^*, and has the value $Re_u = \rho_r^* D^*/\mu_u^* = 10^4$ in the reactants. Re_b is defined accordingly based on ρ_b^* and μ_b^* in the products, and is related to Re_u by $Re_b/Re_u = (\rho_b/\rho_u)^{3/2}$, assuming $\mu \propto T^{1/2}$. Given the above range of values of U, the effective inlet flow Reynolds number $\rho_u^* U^* H^*/\mu_u^*$ is in the range 4400–8400.

Results are obtained for the following combustor dimensions: $L = 4.0$, $H = 1.0$, $x_{min} = -4.0$, $x_{max} = 4.0$. The SLIC/VOF discretization uses a cell size given by $h_F = \Delta x = \Delta y = 0.1$, and a discretized volume source distribution using a maximum of four sources per cell. The vortex method solution uses a discretized sheet length of $h_s = 0.33$ on the domain walls, a sheet layer thickness of $d_s = 0.01$, a vortex element circulation of $\Gamma_\nu^*/D^* U_r^* = 0.028$, and a core radius $\sigma = h_s/\pi$. This discretization is sufficient for resolving the large scales of the flowfield, namely scales larger than the vortex element core radius σ, and flame grid size h_F. Smaller scale structures, such as small flame sheet contortions and vortex eddies, are not resolved. This is deemed an acceptable resolution in the present context, since the object of interest relates to large-scale structures and global flame modulation and dynamics. Validation of the various components of the model has been reported in Najm,[18] Najm and Ghoniem,[6] and Knio.[30]

This exposition is restricted to two heat release cases, with a specified p_{ex} modulation at low frequency, close to the natural wake mode instability of the cavity flowfield at $St = 0.1$. We demonstrate that under low-frequency forcing, the natural flow instability is amplified due to the phase-matched coupling between heat release and flow oscillation leading to flow reversal and flame flashback.

Flow parameters are $\rho_u/\rho_b = 4.0$, and $p_0 = 1.0$. The exit pressure is a cosine function of time with amplitude $p_{mx} = 2.5$, and frequency $f_f = 0.1$. The rate of heat release is varied by changing the normal burning speed from $S_u = 0.025$–0.05. Thus, if the mean flame length were to remain unchanged, then given the two-fold increase of S_u, the mean rate of heat release would be expected to double.

Low Heat Release

The time evolution of the unsteady flowfield is shown in Fig. 2. The number next to each frame indicates nondimensional time. Flow is from left to right. Each vortex element is shown with the local velocity vector drawn from its center. The instantaneous flame contour is shown as a thick solid line. This sequence exhibits one cycle of a large eddy shedding. The flame experiences large amplitude oscillations (flapping) that cause it to intermittently fill the whole dump section, i.e., the trough and the channel above it, propagate slightly into the upstream channel, and then be swept downstream by the flow in a periodic fashion. We will examine the relationship among the inlet flow rate Q_{in} at x_{min}, the pressure in the channel above the upstream step P_{step}, and the vorticity dynamics using Fig. 2 and the time traces of Q_{in} and P_{step} depicted in Figs. 3 and 4.

A typical cycle begins at time $t = 12.0$. At this time, the flame is roughly at its farthest upstream location. The products and the recirculation zone have expanded to fill the entire dump section and the flow rate into the combustor is at its minimum, only slightly larger than zero, while the pressure is falling rapidly. During $t = 12$–14, the flame and vorticity field are convected downstream by the accelerating inlet flow rate, the step pressure reaches a minimum, and the inlet flow rate grows rapidly. A trailing eddy is formed at the step while the leading eddy is being convected against the downstream step. During $t = 14$–16 the flame is dipped strongly into the dump, following the vorticity field, as the trailing eddy grows at the step. The flame moves downstream, being convected along with the leading eddy, such that it is still approximately normal to the streamlines in the incoming flow. These vertical flame shapes, associated with flow acceleration into the combustor, have been observed experimentally under similar conditions (see Vaneveld et al.[5] and Fig. 5b below).

At $t = 16$, the reactants are entrained by the growing trailing eddy, and the flame interface is strongly contorted. The flame in the channel is swept further downstream with the vorticity of the previous large leading eddy. By $t = 17$, the flow rate has reached its maximum while the step pressure is rising rapidly. The trailing eddy is still growing and entraining reactants as it begins to move away from the step. By $t = 18$, the leading eddy has been completely swept away while the trailing eddy is growing, moving downstream, and entraining more reactants. Around $t = 19.5$, the pressure reaches its maximum, $\frac{1}{4}$ period after $(Q_{in})_{max}$, while the flow rate is decreasing rapidly. At $t = 20$, the eddy fills most of the dump and starts to expand upwards, along with the flame interface, as well as upstream and downstream into the channel. Starting around $t = 22$, the cycle is repeated as the flow rate starts to increase again, pushing the products and the large eddy downstream towards the combustor exit. This cycle repeats itself with a period of 10.0, i.e., with frequency $f = 0.1$, $St = f^* D^*/U^* = 0.12$, which corresponds to the forcing frequency f_f. This low-frequency, large-amplitude, flapping of the flame is the precursor to flashback that has been observed extensively in experimental investigations.[3,5,14–17]

The correspondence between the pressure oscillations and the flow structure discussed above is in agreement with the results of Yu et al.[14,15] Their schlieren photographs suggest that the minimum pressure occurs as the trailing eddy starts to form at the upstream step (as at $t = 15$). Similarly, the maximum pressure is found to correspond to a situation where the flame fills the cavity and is still growing to fill the channel (as at $t = 20$). Figures 3 and 4 illustrate the $\frac{1}{4}$ period phase difference between Q_{in} and P_{step}, as observed by Yu et al.[14,15] and Poinsot et al.[35]

The total rate of heat release in the combustor is plotted along with the step pressure and inlet flow rate in Figs. 3 and 4, respectively. We find, as in Yu et al.,[14,15] that the heat release lags the step pressure by roughly $\frac{1}{4}$ of a period, and is roughly $\frac{1}{2}$ period out of phase with the flow rate (see Poinsot et al.[35]). This result is expected since the pressure leads the inlet flow rate by $\frac{1}{4}$ period. The rate of heat release is maximum when Q_{in} is minimum. Hence, the heat release maxima correspond to the flow when the products and the contorted

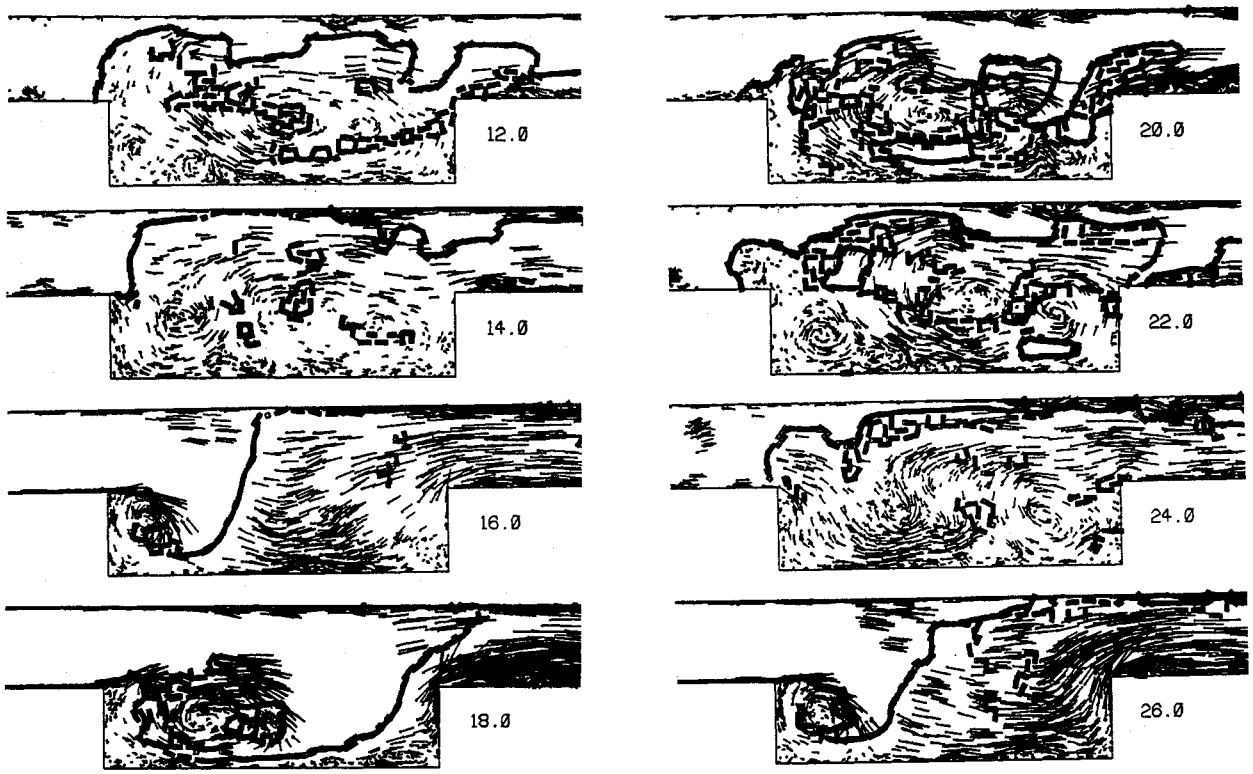

Fig. 2 Sequence of time frames of the combustor flowfield at low heat release (S_u = 0.025, ρ_u/ρ_b = 4.0) and low forcing frequency, illustrating the large amplitude flapping of the flame and the associated large eddy shedding. The number next to each frame indicates nondimensional time. Each vortex element is shown with the local velocity vector drawn from its center. The instantaneous flame contour is shown as a thick solid line.

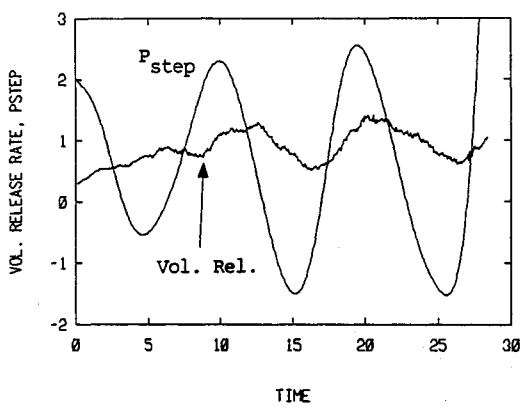

Fig. 3 Time traces of the rate of heat release and the upstream step pressure for the low heat release (S_u = 0.025, ρ_u/ρ_b = 4.0) of Fig. 2.

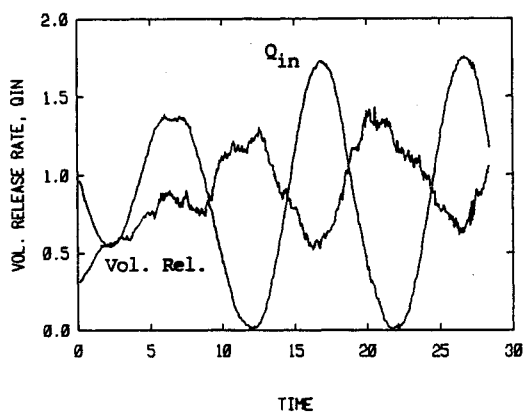

Fig. 4 Time traces of the rate of heat release and the inlet flow rate pressure for the low heat release (S_u = 0.025, ρ_u/ρ_b = 4.0) of Fig. 2. $(Q_{in})_{av}$ = 0.84.

flame interface have expanded to fill the whole dump section, t = 2.0 and 22.0. Moreover, the rate of heat release rises sharply between times 16–20, which corresponds to the time of strong eddy growth and flame contortion.

The fact that the unsteady heat release is only $\frac{1}{4}$ period out of phase with the pressure in the combustor is a significant indicator of the mechanisms governing the combustor dynamics. When the pressure and heat release oscillations are nearly in-phase, sufficient coupling may occur, leading to the growth of disturbances and the amplification of the combustor instability (Rayleigh criterion[10]). We demonstrate this on the present flowfield, under low-frequency pressure forcing, by increasing the burning speed S_u, and observing the resulting combustor dynamics.

High Heat Release

We now discuss the results of the high heat release case, where S_u = 0.05. The flowfield and the flame front are shown in Fig. 5a. We observe dynamics similar to those in the previous case, but with significantly larger amplitude oscillations. Large amplitude oscillations and flow reversal are observed, with the flame propagating further into the upstream channel and exiting the computational domain at x_{min}, as in frame 23.0. We observe less flame contortion and fragmentation at higher S_u. On the other hand, the correspondence between the flow rate and pressure traces, shown in Figs. 6 and 7, respectively, and the flowfield, is similar to that observed before.

The dynamics observed in Fig. 5a, including the liftoff of the flame in the upstream boundary layer and the large amplitude flame flapping, are similar to the schlieren pictures of the flowfield in the "chucking" mode observed in the experiment by Vaneveld et al.,[5] as shown in Fig. 5b. The characteristic Strouhal number measured in this experiment was St = 0.15. The sequence of schlieren images exhibits strong periodic flame flapping, along with the characteristic vertical flame shapes mentioned above, as observed in Figs. 2 and 5a. Similarly, Keller et al.[4] show experimental pictures from a

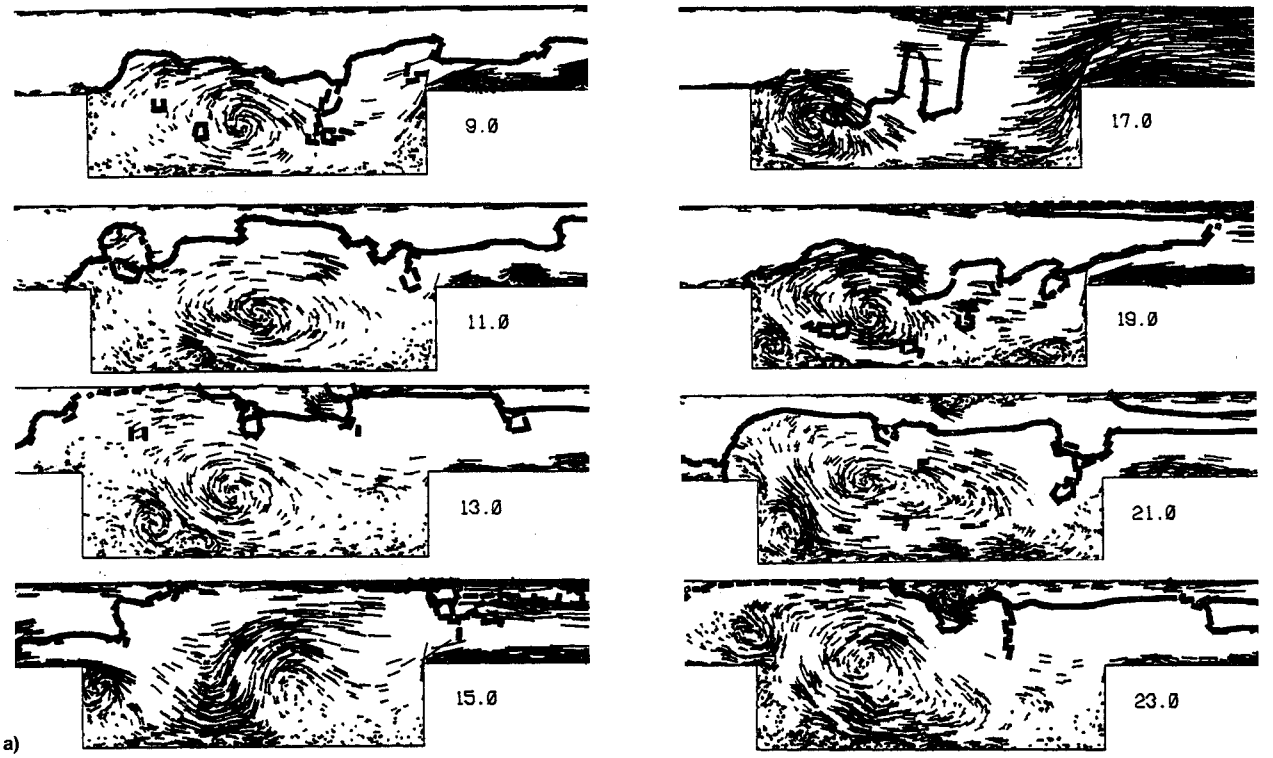

a)

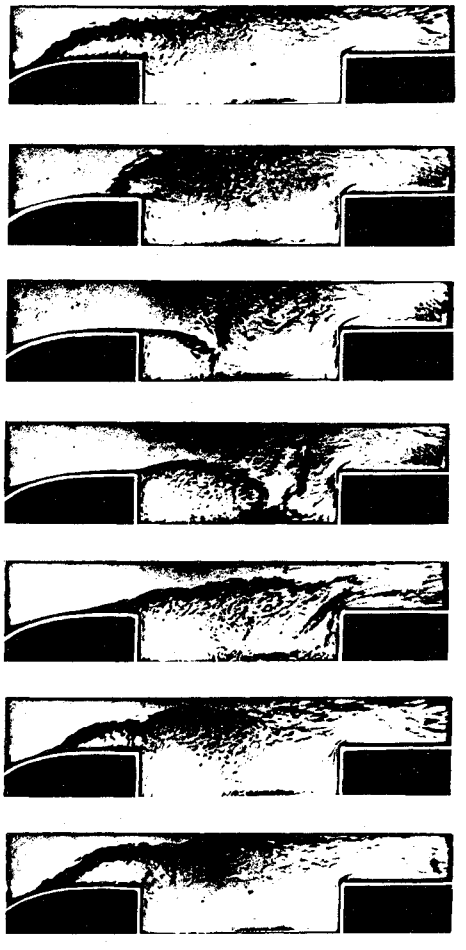

b)

Fig. 5 a) Sequence of time frames of the combustor flowfield at high heat release ($S_u = 0.05$, $\rho_u/\rho_b = 4.0$) and low forcing frequency, illustrating the large amplitude flapping of the flame and the associated large eddy shedding and flow reversal. The number next to each frame indicates nondimensional time. Each vortex element is shown with the local velocity vector drawn from its center. The instantaneous flame contour is shown as a thick solid line. b) Experimental schlieren photographs exhibiting large-scale, low-frequency flame flapping in a premixed dump combustor, from Vaneveld et al.[5] Inlet flow velocity: 9.12 m/s ($Re = 1.5 \times 10^4$). Time interval between frames: 3 ms.

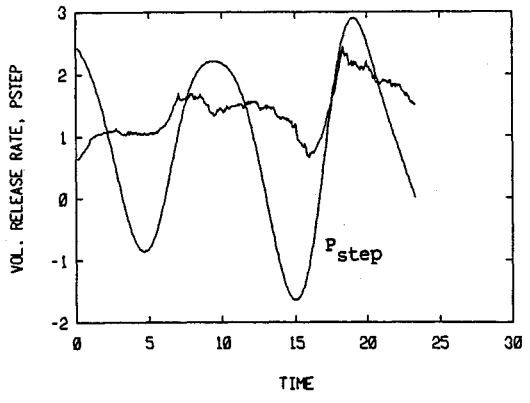

Fig. 6 Time traces of the rate of heat release and the upstream step pressure, for the high heat release (S_u = 0.05, ρ_u/ρ_b = 4.0) case of Fig. 5a.

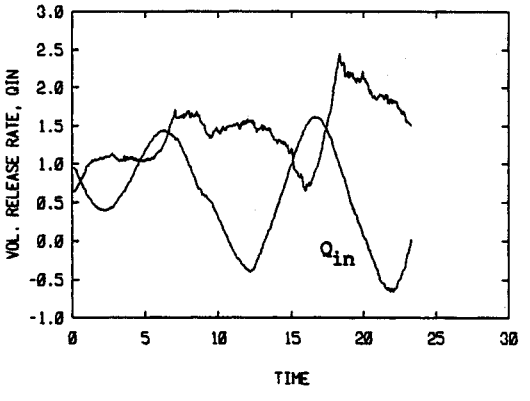

Fig. 7 Time traces of the rate of heat release and the inlet flow rate, for the high heat release (S_u = 0.05, ρ_u/ρ_b = 4.0) case of Fig. 5a. $(Q_{in})_{av}$ = 0.57.

step-dump combustor flow that exhibits large amplitude oscillation as is observed here, with St = 0.11. Again, we see the same cyclic flapping of the flame and vorticity field occurring at $St = \mathcal{O}(0.1)$.

The period of the recirculation zone eddy shedding is roughly 10, corresponding to the forcing frequency f_f = 0.1. The strong oscillation of the pressure within the combustor causes significant flow reversal at the inlet plane, with Q_{in} reaching a minimum of −0.6. Thus, increasing S_u to 0.05 has increased the amplitude of oscillations in the flowfield. The spectra of Q_{in} and P_{step} exhibit a dominant peak at f = 0.1; corresponding to St = 0.17, this is the forcing frequency. Again we find that the flow dynamics are amplified at the forcing St when the latter is close to 0.1. The phase difference between the P_{step} and Q_{in} traces is observed to be $\frac{1}{4}$ of the period, as in the low heat release case.

The heat release is more closely in-phase with the pressure oscillation than in the previous case. Increasing S_u tends to increase the amplitude of the heat release rate and to decrease the phase lag between it and the pressure oscillation. Both of these factors tend to amplify the combustor dynamics as illustrated by the evidence of flow reversal in the present case. The rate of heat release, shown in Figs. 6 and 7, rises sharply for time 16–18, which corresponds to the period of strong entrainment into the large eddy. It reaches a higher maximum in the second cycle indicating the formation of a stronger eddy. In this second cycle, the heat release and the pressure are seen to rise simultaneously, with the heat release peak occuring slightly before the pressure peak and staying high for the duration of the latter peak. As indicated above, this phase relationship leads to the amplification of the combustor oscillations. The heat release rate, being almost in phase with the pressure oscillation, is $\frac{1}{4}$ period out of phase with the inlet flow rate oscillation.

We have thus shown that under conditions of low-frequency forcing, when the forcing frequency is close to the natural frequency of the combustor, as defined by the shedding frequency of the recirculation zone $St = f^*D^*/U^* = \mathcal{O}(0.1)$, increasing the rate of heat release causes the recirculation zone instability and the resulting pressure and flow rate oscillations to be amplified. As the flow slows down, or reverses, at the inlet section, the flame flashes back into the upstream channel.

Conclusions

A numerical model is developed to study the dynamics of reacting flow in a dump combustor. The random vortex method along with an interface advection and propagation flame model are used to compute the low Mach number flow in a two-dimensional compact combustor. The pressure is incorporated in the model in order to provide the crucial coupling between the combustor flowfield and the inlet flow system. The overall system is forced by specifying the exit pressure. The imposed exit pressure oscillation represents possible natural pressure oscillations in the overall combustion system. The inlet flow rate is determined by the inlet pressure, computed from the flowfield, and the exit pressure.

Results show that when the exit pressure is forced at low frequency, close to the combustor natural frequency, the recirculation zone instability is amplified as the rate of heat release is increased, ultimately leading to flow reversal and flame flashback.

These results agree with the instability requirement dictated by the Rayleigh criterion,[10] which states that sufficient coupling may occur between the pressure and the heat release oscillations leading to the growth of disturbances only when these oscillations are in phase. When the pressure is modulated at high frequency, its fluctuation component at the low natural frequency is inhibited and cannot be amplified by the heat release, which oscillates at the low natural frequency.[18] On the other hand, when the exit pressure is modulated at low frequency, close to the combustor natural frequency, this amplification is possible. As we have seen, this amplification is enhanced by both the increased amplitude of the rate of heat release and the smaller phase difference between the heat release oscillation and the pressure oscillation.

Acknowledgments

This work is supported by the Air Force Office of Scientific Research Grant AFOSR 84-0536, the National Science Foundation Grant CBT8709465, and the Department of Energy Grant DE-FG0487AL44875. Computer support is provided by the John von Neumann National Supercomputer Center, Princeton, New Jersey.

References

[1]Lewis, B., and Von Elbe, G., *Combustion, Flame, and Explosions of Gases*, 2nd ed., Academic Press, New York, 1961, pp. 228–261, 439.

[2]Plee, S. L., and Mellor, A. M., "Review of Flashback Reported in Prevaporizing/Premixing Combustors," *Combustion and Flame*, Vol. 32, No. 1, 1978, pp. 193–203.

[3]Gangi, A. R., and Sawyer, R. F., "An Experimental Study of the Flow Field and Pollutant Formation in a Two-Dimensional, Premixed, Turbulent Flame," AIAA Paper 79-0017, Jan. 1979.

[4]Keller, J. O., Vaneveld, L., Korschelt, D., Hubbard, G. L., Ghoniem, A. F., Daily, J. W., and Oppenheim, A. K., "Mechanism of Instabilities in Turbulent Combustion Leading to Flashback," AIAA Paper 81-0107, Jan. 1981.

[5]Vaneveld, L., Hom, K., and Oppenheim, A. K.,"Secondary Effects in Instabilities Leading to Flashback," AIAA Paper 82-0037, Jan. 1982.

[6]Najm, H. N., and Ghoniem A. F., "Numerical Simulation of the Convective Instability in a Dump Combustor," *AIAA Journal*, Vol. 29, No. 6, 1991, pp. 911–919.

[7]Menon, S., and Jou, W. H., "Simulations of Ramjet Combustor

Flow Fields, Part I—Numerical Model, Large-Scale and Mean Motions," AIAA Paper 87-1421, June 1987.

[8]Driver, D. M., Seegmiller, H. L., and Marvin, J. G., "Time-Dependent Behaviour of a Reattaching Shear Layer," *AIAA Journal*, Vol. 25, No. 7, 1987, pp. 914–919.

[9]Eaton, J. K., and Johnston, J. P., "Low Frequency Unsteadiness of a Reattaching Turbulent Shear Layer," *Third International Symposium on Turbulent Shear Flows*, edited by L. J. Bradbury, F. Durst, B. Launder, F. Schmidt, and H. Whitelaw, Springer-Verlag, Berlin, 1981, pp. 162–170.

[10]Rayleigh, J. W. S., *The Theory of Sound: Vol. II*, Dover, New York, 1945.

[11]Smith, D., and Zukoski, E., "Combustion Instability Sustained by Unsteady Vortex Combustion," AIAA Paper 85-1248, July 1985.

[12]Kailasanath, K., Gardner, J. H., Boris, J. P., and Oran, E. S., "Acoustic-Vortex Interactions and Low Frequency Oscillations in Axisymmetric Combustors," AIAA Paper 87-0165, Jan. 1987.

[13]Jou, W.-H., and Menon, S., "Simulations of Ramjet Combustor Flow Fields, Part II—Origin of Pressure Oscillations," AIAA Paper 87-1422, June 1987.

[14]Yu, K., Lee, S., Trouve, A., Stewart, H. E., and Daily, J. W., "Vortex-Nozzle Interactions in Ramjet Combustors," AIAA Paper 87-1871, June–July 1987.

[15]Yu, K., Trouve, A., Keanini, R., and Bauwens, L.,"Low Frequency Pressure Oscillations in a Model Ramjet Combustor—The Nature of Frequency Selection," AIAA Paper 89-0623, Jan. 1989.

[16]McManus, K. R., Vandsburger, U., and Bowman, C. T., "Modification of Combustion Characteristics of a Dump Combustor Using Shear Layer Excitation," Mechanical Engineering Dept. Rept., Stanford Univ., Stanford, CA, 1987.

[17]Schadow, K., Wilson, K., Crump, J., Foster, J., and Gutmark, E., "Interaction Between Acoustics and Subsonic Ducted Flow with Dump," AIAA Paper 84-0530, Jan. 1984.

[18]Najm, H. N., "Numerical Investigation of the Instability of Premixed Dump Combustors," Ph.D. Dissertation, Dept. of Mechanical Engineering, Massachusetts Inst. of Technology, Cambridge, MA, June 1989.

[19]Najm, H. N., and Ghoniem, A. F., "Modeling Combustion Pulsation Due to Flow-Flame Interactions in Vortex-Stabilized Premixed Flames," International Symposium on Pulsating Combustion, Monterey, CA, Aug. 1991.

[20]Fristrom, R. M., and Westenberg, A. A., *Flame Structure*, McGraw-Hill, New York, 1965.

[21]Peters, N., "Laminar Flamelet Concepts in Turbulent Combustion," *21st Symposium (International) on Combustion/The Combustion Institute*, 1986, pp. 1231–1259.

[22]Sivashinsky, G. I., "Hydrodynamic Theory of Flame Propagation in an Enclosed Volume," *Acta Astronautica*, Vol. 6, 1979, pp. 631–645.

[23]Markstein, G. H., "Perturbation Analysis of Stability and Response of a Plane Flame Front," *Non-Steady Flame Propagation*, edited by G. Markstein, Pergamon, Oxford, England, UK, 1964, pp. 15–73.

[24]Hayes, W. D., "The Vorticity Jump Across a Gas Dynamic Discontinuity,"*Journal of Fluid Mechanics*, Vol. 2, 1957, pp. 595–600.

[25]Batchelor, G. K., *An Introduction to Fluid Mechanics*, Cambridge Univ. Press, Cambridge, England, UK, 1985.

[26]Chorin, A. J., "Numerical Study of Slightly Viscous Flow," *Journal of Fluid Mechanics*, Vol. 57, Pt. 4, 1972, pp. 785–796.

[27]Chorin, A. J., "Vortex Sheet Approximation of Boundary Layers," *Journal of Computational Physics*, Vol. 27, 1978, pp. 428–442.

[28]Ghoniem, A. F., and Ng, K., "Numerical Study of the Dynamics of a Forced Shear Layer," *Physics of Fluids*, Vol. 30, No. 3, 1987, pp. 706–721.

[29]Ghoniem, A. F., Chorin, A. J., and Oppenheim, A. K., "Numerical Modelling of Turbulent Flow in a Combustion Tunnel," *Philosophical Transactions of the Royal Society of London*, A, Vol. 304, 1982, pp. 303–325.

[30]Knio, O. M., "Low Mach Number Simulation of Combustion in Closed Chambers," M.S. Thesis, Mechanical Engineering, Massachusetts Inst. of Technology, Cambridge, MA, 1984.

[31]Noh, W. T., and Woodward, P., "SLIC (Simple Line Interface Calculation)," *Proceedings of the 5th International Conference on Numerical Methods in Fluid Dynamics*, Springer-Verlag, Berlin, 1976, pp. 330–340.

[32]Hirt, C., and Nichols, B., "Volume of Fluid (VOF) Method for the Dynamics of Free Boundaries," *Journal of Computational Physics*, Vol. 39, 1981, pp. 201–225.

[33]Trefethen, L. N., "Numerical Computation of the Schwartz-Christoffel Transformation," Computer Science Dept., Stanford Univ. STAN-CS-79-710, Stanford, CA, 1979.

[34]Emmons, H. W., "Highspeed Aerodynamics and Jet Propulsion," *Fundamentals of Gas Dynamics*, edited by H. W. Emmons, Vol. 3, Princeton Univ. Press, Princeton, NJ, 1958, Chap. 2.

[35]Poinsot, T. J., Trouve, A. C., Veynante, D. P., Candel, S. M., and Esposito, E. J., "Vortex-Driven Acoustically Coupled Combustion Instabilities," *Journal of Fluid Mechanics*, Vol. 177, 1987, pp. 265–292.